physchem

MDPI

Article

Cyclic Voltammetry Study of *Closo*-Ruthenacarboranes

Ivan D. Grishin *, Anastasia M. Zimina and Alexander A. Kaltenberg

Department of Chemistry, Lobachevsky State University of Nizhny Novgorod, 23 Gagarin Prosp., 603950 Nizhny Novgorod, Russia

* Correspondence: grishin_i@ichem.unn.ru

Abstract: Electrochemical properties of transition metal complexes are important parameters that should be considered for the successful application of these compounds in catalytic reactions. The proper choice of ligands and the type of its coordination allow the construction of a catalyst with high performance. The reversibility of complex oxidation is a prerequisite for successful participation in redox catalysis, while the potential values correlate with the rate of the process and necessary catalyst loading. This work summarizes the results of the exploration of a series of ruthenium carborane complexes based on the *nido*-C_2B_9 ligand obtained in our group by cyclic voltammetry and describes the found correlations. The knowledge of the electrochemical properties of the studied ruthenacarboranes is required for the optimization of its structure for successful catalysis of Atom Transfer Radical Polymerization or other applications. It was found that the value of the potential of reversible Ru(II)-Ru(III) transition may vary from −0.501 to 0.389 V versus $Fc|Fc^+$ couple, depending on the nature of auxiliary phosphine, halogen or nitrile ligand, natural bite angle of κ^2-diphosphine ligand and the presence of alkyl substituents in the carborane cage. The further oxidation towards formal Ru(IV) may be reversible or not depending on the complex structure. The found trends are in good agreement with the earlier performed findings in the field of coordination chemistry and should be considered as a tool for obtaining of complexes suitable for catalytic applications.

Keywords: ruthenacarboranes; cyclic voltammetry; electrochemistry; ruthenium complexes; diphosphines

Citation: Grishin, I.D.; Zimina, A.M.; Kaltenberg, A.A. Cyclic Voltammetry Study of *Closo*-Ruthenacarboranes. *Physchem* **2023**, *3*, 232–243. https://doi.org/10.3390/physchem3020016

Academic Editors: Michael E. G. Lyons and José Solla Gullón

Received: 7 February 2023
Revised: 21 April 2023
Accepted: 17 May 2023
Published: 19 May 2023

1. Introduction

Carborane complexes of transition metals based on *nido*-C_2B_9 ligand are isolobal analogs of cyclopentadienyl derivatives that have found a wide application in catalysis, including isomerization, hydrogenation, radical addition [1–3] and other spheres of chemistry [4–6]. Due to the double negative charge and delocalization of electron density, carborane ligand is capable to stabilize transition metals in high oxidation states and makes possible the formation of intermediates in catalytic cycles [1,4]. The introduction of substituents at carbon or boron atoms of carborane cage affects steric and electronic parameters of metallacarborane and may be considered as a tool for tuning a complex for its application in catalysis. Electrochemical properties of complexes of transition metals are used for predicting their catalytic performance, as the reversibility of the electron transfer and the value of potential are parameters that usually correlate with the results of catalytic tests [7,8]. It was shown that the redox potential of ruthenium ethylenediaminetetraacetate complexes determined by auxiliary ligands correlates with its electrocatalytic performance [9]. A similar observation was done for Ru(II)-polypyridine complexes with alkynyl Schiff base ligands [10]. The potential of Ru(II)-Ru(III) transition plays a key role in the activation of the ruthenium anticancer prodrugs in vivo [11] as well in light-harvesting applications [12] and light-emitting diodes [13]. Thus, electrochemical properties of complexes are widely explored and their correlations with structure and properties are carefully analyzed in numerous reviews and original papers [14–18].

Closo-ruthenacarboranes based on *nido*-C_2B_9 ligands are known as effective catalysts of Atom Transfer Radical Polymerization (ATRP) [19,20], a powerful tool for obtaining well-defined polymers [21,22]. Among the known *closo*-ruthenacarboranes 18-e complexes of Ru(II), 17-e complexes of Ru(III), and 18-e complexes of Ru(IV) are distinguished. The first ones contain three 2-e neutral monodentate ligands or corresponding polydentate ligands bounded to RuC_2B_9 moiety. Such compounds may be electrochemically oxidized to Ru(III) species. The reversibility of the process depends on the structure of the complex. Stable 17-e complexes of Ru(III) have a similar structure but are characterized by the presence of only two neutral σ-ligands while the last coordination site is occupied by a halogen. They may be reduced to corresponding Ru(II) anions. In 18-e complexes of Ru(IV), an additional hydride ligand is bounded to the ruthenium atom. Such complexes are characterized by unexpectable high stability but may be converted to the mentioned Ru(III) species in the presence of free radicals or its precursors.

The recent review of Teixdor [23] shows the wide diversity of redox potential values possible for bis(dicarbollide) clusters of cobalt, nickel, and iron depending on the nature substituents in boron cages. At the same time the similar generalization of the properties ruthenium derivatives was not found in the literature although in may be useful for boron cluster scientists and researchers working in the area of ruthenium complexes. This work summarizes the results of electrochemical exploration of a series of ruthenium carborane complexes first obtained in our group by cyclic voltammetry, describes the found correlations and provides the ways of tuning complex potential by changing ligand environment.

2. Materials and Methods

Ruthenium complexes were synthetized according to the methods described in the references provided in Tables 1 and 2. 1,2-dichloroethane and acetonitrile (Sigma-Aldrich, St. Louis, MO, USA) were distilled over calcium hydride prior to use. *n*-Bu_4NPF_6 and AgCl were purchased from Sigma-Aldrich and used as received.

Table 1. The results of cyclic voltammetry studies of 18-e *closo*-ruthenacarboranes *.

Complex	L	R_1, R_2	Ep_a	[Ref]
1a	Cl	−H, −H	1.10	[9]
1b	Cl	−H, $-CH_3$	1.01	[10]
1c	Cl	−H, $-C_4H_9$	1.08	[10]
1c	Cl	$-CH_3$, $-CH_3$	0.96	[10]
1d	Br	−H, −H	1.02	[16]

* Solvent: 1,2-dichloroethane with 0.2 M n-Bu_4NPF_6 as the supporting electrolyte. [Ru] = 0.003 M. Scan rate: 0.1 V/s. The values are referred to ferrocene as internal standard.

Table 2. The results of cyclic voltammetry studies of *closo*-ruthenacarboranes *.

Complex	Type	X	L	R_1, R_2	Ru(II)–Ru(III), V			Ru(III)–Ru(IV), V			[Ref]
					Ep_a	Ep_c	$E_{1/2}$	Ep_a	Ep_c	$E_{1/2}$	
2a	17-e	CH_2	Cl	−H, −H	−0.398	−0.480	−0.439	0.548 **	–	–	[24]
2b	17-e	$(CH_2)_2$	Cl	−H, −H	−0.297	−0.367	−0.332	0.677 **	–	–	[25]
2c	17-e	$(CH_2)_3$	Cl	−H, −H	−0.279	−0.343	−0.311	0.683 **	–	–	[25]
2d	17-e	$(CH_2)_4$	Cl	−H, −H	−0.251	−0.332	−0.292	0.721 **	–	–	[19]
2e	17-e	$(CH_2)_5$	Cl	−H, −H	−0.245	−0.318	−0.282	0.720 **	–	–	[26]
2f	17-e	o-C_6H_4	Cl	−H, −H	−0.312	−0.399	−0.356	0.779 **			[24]
2g	17−e	$(CH_2)_2$	Br	−H, −H	−0.276	−0.352	−0.314	0.691 **	–	–	[27]
2h	17-e	$(CH_2)_3$	Br	−H, −H	−0.245	−0.320	−0.282	0.756 **	–	–	[27]
2j	17-e	$(CH_2)_4$	Br	−H, −H	−0.212	−0.291	−0.251	0.805 **	–	–	[27]
2k	17-e	$(CH_2)_4$	Cl	−H, $-C_4H_9$	−0.343	−0.410	−0.377	0.725 **	–	–	[20]
2l	18-e	CH_2	CH_3CN	−H, −H	0.206	0.138	0.172	–	–	–	[24]
2m	18-e	$(CH_2)_2$	CH_3CN	−H, −H	0.290	0.190	0.240	0.954 **	–	–	[28]
2n	18-e	$(CH_2)_4$	CH_3CN	−H, −H	0.367	0.280	0.324	1.166 **	–	–	[29]
2o	18−e	$(CH_2)_4$	C_6H_5CN	−H, −H	0.368	0.283	0.326	0.935 **	–	–	[30]
2p	18-e	$(CH_2)_4$	CH_2=CHCN	−H, −H	0.366	0.273	0.320	0.848 **	–	–	[30]
2q	18-e	CH_2	PPh_3	−H, −H	0.432	0.345	0.389	–	–	–	[24]
2r	18-e	o-C_6H_4	CH_3CN	−H, −H	0.320	0.206	0.263	–			[24]

Table 2. *Cont.*

Complex	Type	X	L	R_1, R_2	Ru(II)–Ru(III), V			Ru(III)–Ru(IV), V			[Ref]
					Ep_a	Ep_c	$E_{1/2}$	Ep_a	Ep_c	$E_{1/2}$	
3a	17-e	$(CH_2)_3$	Cl	−H, −H	−0.357	−0.426	−0.391	0.624 **	–	–	[31]
3b	17-e	$(CH_2)_4$	Cl	−H, −H	−0.316	−0.393	−0.355	0.683 **	–	–	[19]
3c	17-e	$(CH_2)_5$	Cl	−H, −H	−0.274	−0.345	−0.310	0.677 **	–	–	[26]
3d	17-e	$(CH_2)_3$	Br	−H, −H	−0.285	−0.351	−0.318	0.619 **	–	–	[27]
3e	17-e	$(CH_2)_4$	Br	−H, −H	−0.277	−0.344	−0.311	0.610 **	–	–	[27]
3f	17-e	$(CH_2)_5$	Br	−H, −H	−0.254	−0.323	−0.288	0.716 **	–	–	[27]
3g	17-e	$(CH_2)_4$	Cl	−H, $-CH_3$	−0.383	−0.463	−0.423	0.615 **	–	–	[32]
3h	17-e	$(CH_2)_4$	Cl	$-CH_3$, $-CH_3$	−0.417	−0.488	−0.452	0.570 **	–	–	[32]
3i	18-e	$(CH_2)_4$	CH_3CN	−H, −H	0.284	0.211	0.248	0.790 **	–	–	[28]
3j	18-e	$(CH_2)_4$	C_6H_5CN	−H, −H	0.285	0.204	0.244	0.690 **	–	–	[30]
3k	18-e	$(CH_2)_4$	CH_2=CHCN	−H, −H	0.291	0.204	0.248	0.680 **	–	–	[30]
3l	18-e	$(CH_2)_2$	PPh_3	−H, −H	0.425	0.329	0.377	0.905 **	–	–	[28]
3m	18-e	$(CH_2)_3$	PPh_3	−H, −H	0.450	0.387	0.418	1.100 **	–	–	[31]
3n	18-e	$(CH_2)_4$	PPh_3	−H, −H	0.275	0.207	0.241	0.802 **	–	–	[26]
4a	17-e	$(CH_2)_3$	Cl	–	−0.461	−0.542	−0.501	0.517 **	–	–	[25]
4b	17-e	$(CH_2)_4$	Cl	–	−0.426	−0.497	−0.461	0.553 **	–	–	[25]
5a	17-e	$(CH_2)_3$	Cl	−H, −H	−0.393	−0.458	−0.426	0.575	0.510	0.543	[19]
5b	17-e	$(CH_2)_4$	Cl	−H, −H	−0.358	−0.428	−0.393	0.627	0.551	0.589	[19]
5c	17-e	$(CH_2)_5$	Cl	−H, −H	−0.279	−0.348	−0.313	0.637	0.551	0.594	[26]
5d	17-e	$(CH_2)_4$	Br	−H, −H	−0.346	−0.414	−0.380	0.634	0.560	0.597	[27]
5e	17-e	$(CH_2)_4$	Cl	−H, $-CH_3$	−0.419	−0.510	−0.464	0.601	0.509	0.555	[32]
5f	17-e	$(CH_2)_4$	Cl	$-CH_3$, $-CH_3$	−0.454	−0.540	−0.497	0.571	0.488	0.530	[32]
5g	18-e	$(CH_2)_4$	CH_3CN	−H, −H	0.164	0.093	0.128	0.763	0.685	0.724	[28]
6a	17-e	−H, −H	Cl	–	−0.274	−0.350	−0.312	0.702 **	–	–	[33]
6b	17-e	NH	Cl	–	−0.280	−0.360	−0.320	0.471 **	–	–	[33]
6c	17-e	$C(CH_3)_2$	Cl	–	−0.298	−0.369	−0.333	0.800 **	–	–	[33]
6d	18-e	−H, −H	CH_3CN	–	0.395	0.300	0.348	–	–	–	[33]
6e	18-e	NH	CH_3CN	–	0.360 **	–	–	–	–	–	[33]
6f	18-e	$C(CH_3)_2$	CH_3CN		0.331	0.242	0.286	–	–	–	[33]
7	18-e	–	–	–	0.421	0.332	0.376	0.933	0.822	0.877	[34]
8	18-e	–		–	0.615 **	–	–	–	–	–	[34]
9	18-e	–	–	–	0.560 **	–	–	–	–	–	[34]
10	17-e	–	–	–	−0.465	−0.345	−0.405	0.513 **	–	–	[34]
11a	18-e	−H	–		−0.055	−0.124	−0.089	–	–	–	[35]
11b	18-e	$-CH_3$	–	–	0.043	−0.031	0.006	–	–	–	[35]
11c	18-e	$-C_2H_5$	–	–	0.074	−0.015	0.029	–	–	–	[35]
11d	18-e	$-CH(CH_3)_2$	–	–	−0.005	−0.077	−0.041	–	–	–	[35]
11e	18-e	$-C(CH_3)_3$	–	–	0.018	−0.045	−0.014	–	–	–	[35]

* Solvent: 1,2-dichloroethane with 0.2 M n-Bu_4NPF_6 as the supporting electrolyte. [Ru] = 0.003 M. Scan rate: 0.1 V/s. The values are referred to ferrocene as internal standard. ** irreversible oxidation.

Electrochemical measurements were performed with an IPC Pro-M potentiostate (Volta, Saint-Petersburg, Russia) with the digital recording of the results. The studies were performed in 1,2-dichloroethane with 0.2 M *n*-Bu_4NPF_6 as the supporting electrolyte. The measurements were carried out under Ar atmosphere in a conventional three-electrode cell (3 mL) with a Pt disk (0.8 mm in diameter) as the working electrode, a Pt wire as the counter electrode and Ag/0.01 M $AgNO_3$ plus 0.2 M *n*-Bu_4NPF_6 in acetonitrile as the reference electrode [36]. Pt electrodes were treated with concentrated sulfochromic mixture and washed with deionized water before use.

In a typical experiment 232 mg (0.6 mmol) of *n*-Bu_4NPF_6 were dissolved in 3 mL of 1,2-dichloroethane, and a baseline signal was recorded to certain the absence of impurities on the electrode surface and in solution. After that 0.009 mmol (ca 6–9 mg) of ruthenacarborane was added and the CV curves were recorded after full dissolution of the complex.

Ferrocene was used as an internal standard [32]. A 1–2 mg of ferrocene was added to the electrochemical cell after the study of each complex. In the case of exploration compounds **11a–e** external calibration of electrode relative ferrocene was performed.

3. Results

In the present work, a cyclic voltammetry study of 60 *closo*-ruthenacarboranes is discussed, and the correlations between complex structures and their electrochemical properties are established. The structures of the studied compounds are presented in Figure 1.

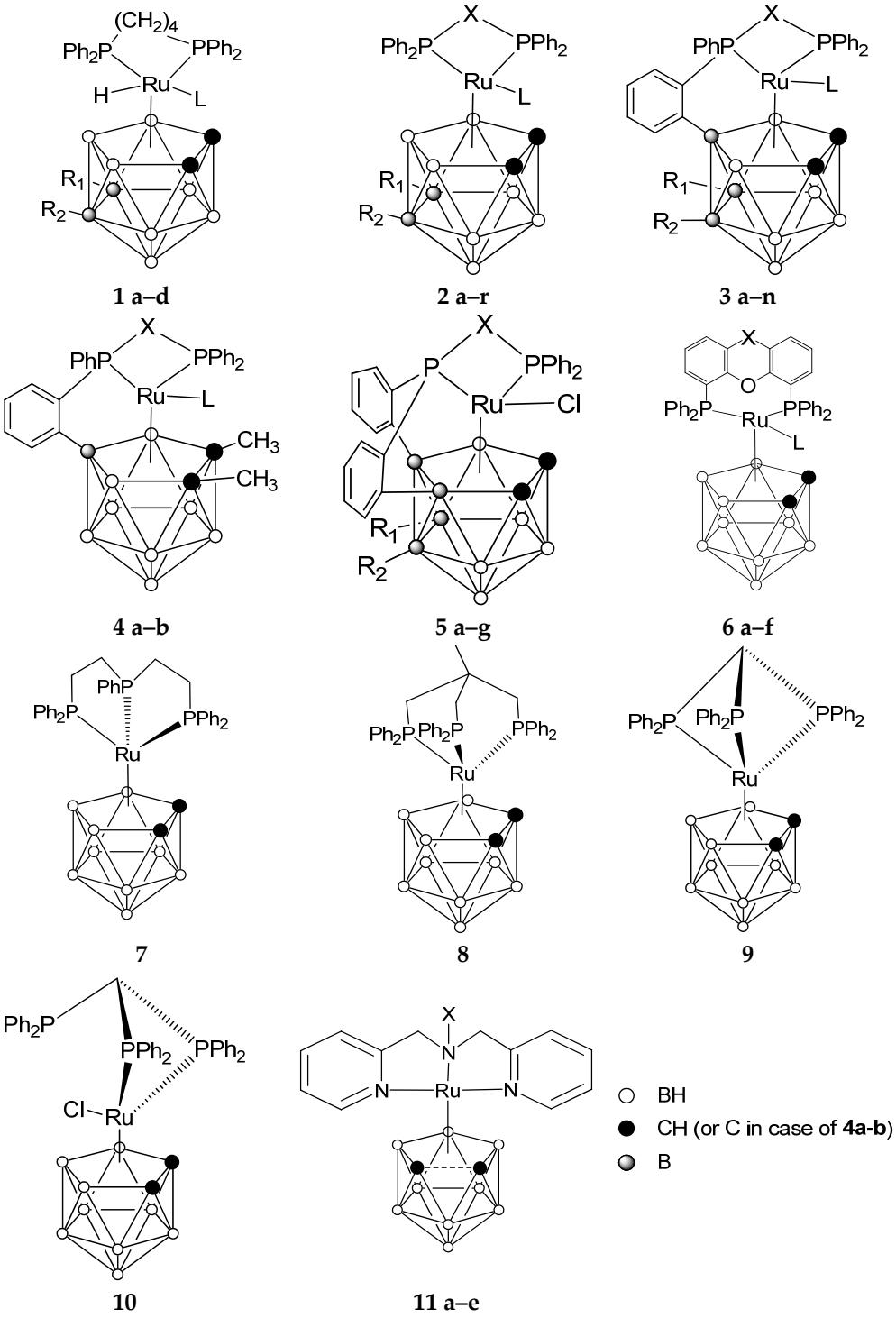

Figure 1. The structures of the studied ruthenacarboranes.

Complexes **1a**–**1d** are air-stable 18-e compounds. The formal oxidation state of ruthenium is +4. These compounds undergo irreversible oxidation with Ep_a 1.0–1.1 V versus ferrocene. The CVA curve recorded for complex **1a** is represented in Figure 2. The other curves are similar. According to the data provided in Table 1, the presence of alkyl sub-

stituents in the lower belt of the carborane cage results in a decrease in the value of the potential at which oxidation starts. A bromine-containing complex **1d** is oxidized at a slightly lower potential than its chlorine-based analog. High values of oxidation potentials correlate with the high stability of these compounds in air or solution observed earlier [19].

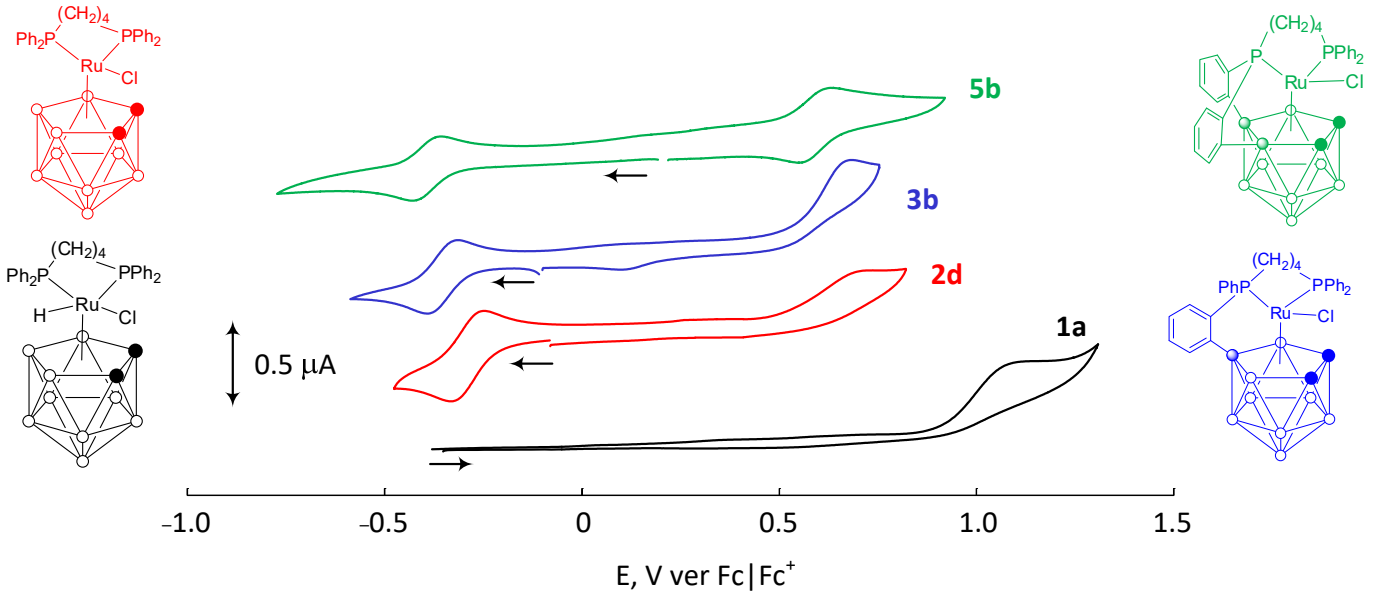

Figure 2. Typical CVA curves recorded for 18-e complexes of Ru(IV) (**1a**) and 17-e complexes of Ru(III) (**2d**, **3b**, **5b**) in 1,2-dichloroethane with 0.2 M n-Bu_4NPF_6 as the supporting electrolyte at 25 °C. [Ru] = 0.003 M. Scan rate: 0.1 V/s.

Complexes **2a**–**2k** are examples of stable paramagnetic 17-e complexes of ruthenium (III). Some of them may be obtained by abstracting hydrogen atoms from complexes **1a**–**1d** [19,26]. The reversible reduction of complex **2d** is observed in Figure 2, while the CVA curves for other compounds have similar nature. Due to the presence of a semi-occupied orbital, these compounds attach additional electrons in the reversible reduction process. In this case, stable 18-e anions similar to the known [3-Cl-3,3-$(PPh_3)_2$-*closo*-$C_2B_9H_{11}$]$^-$ [37] are formed on the electrode surface. These anions may be converted back to 17-e species in the reverse oxidation process.

The analysis of the data provided in Table 2 allows us to conclude that the increase in the number of methylene units in the diphosphine ligand results in a gradual increase of potential value. This tendency is observed as for chlorine-containing complexes **2a**–**2e**, so for its bromine-containing counterparts **2g**–**2j**. It should be noted that the difference between $E_{1/2}$ of complexes distinguished in one CH_2 unit increases with the decrease of the length of methylene chain. Taking into account that donating abilities of the studied bis(diphenylphospino)alkane ligands are similar, the observed differences may be explained by steric factors and bite angles of diphosphine ligands. This proposition is confirmed by similarity of $E_{1/2}$ values measured for **2f** based on 1,2-bis-(diphenylphosphino)benzene and **2b** containing 1,2-bis-(diphenylphosphino)ethane with close bite angles [38]. The similar tendency is observed for complexes **2m** and **2r**.

The exchange of chlorine for bromine atoms leads to the increase of Ru(II)-Ru(III) transition potential by 0.02–0.04 V. The introduction of n-butyl substituent results in decrease of redox potential of **2k** by 0.08 V relative its analogue **2d** indicating donating ability of butyl substituent.

Oxidation of 17-e species **2a**–**2k** proceeds fully irreversible as shown for **2d** in Figure 2. The value of Ep_a tends to increase with the increase of the number of methylene units in diphosphine ligand, the bromine-containing complexes are characterized by higher Ep_a values, similarly as it was observed for Ru(II)-Ru(III) transition.

Compounds **2l**–**2r** contain neutral monodentate ligand instead of halogen and are diamagnetic 18-e complexes of ruthenium (II). Thus, the corresponding Ru(II)/Ru(III)

transition should be considered as oxidation. It also proceeds reversible but at higher potential values (0.1–0.4 V versus ferrocene) in comparison with the earlier discussed 17-e species. The increase of the oxidation potential is observed in row **2l**–**2n** with the increase of the length of the methylene bridge in the diphosphine ligand and its bite angle. Interestingly complexes **2n**–**2p** with different nitrile ligands (acetonitrile, benzonitrile, and acrylonitrile) have similar redox potentials which do not depend on the nature of the alkyl or aryl radical. At the same time the exchange of nitrile by triphenylphosphine results in the increase of the potential of Ru(II)/Ru(III) transition by 0.23 V (**2l** and **2q**). The redox behavior of **2l** and **2q** can be explained by the predominant tendency of phosphine ligands on the redox potential of ruthenacarborane.

Further oxidation of **2m**–**2p** to Ru(IV) species proceeds irreversibly. The measured Ep_a values are higher than for the similar 17-e species. In the cases of compounds **2l**, **2q,** and **2r** no second oxidation waves were observed in the studied range of potentials. It should be noted that the Ep_a value for Ru(III)-Ru(IV) transition for nitrile-based complexes **2n**–**2p** depends on the structure of the auxiliary ligand. The acrylonitrile-based complex **2p** with a double bond in its structure is characterized by the lowest oxidative stability, while the highest potential was observed for its saturated acetonitrile-based analog.

A key feature of compounds **3a**–**3n** and **4a**–**4b** is the presence of covalent bond between carborane and diphosphine ligands. This bond should increase the stability of complexes and prevent its full decomposition. Complexes **3a**–**3h** are paramagnetic 17-e species while compounds **3i**–**3n** are diamagnetic. Electrochemical properties of such complexes are generally similar to those discussed earlier for compounds **2a**–**2r**. These compounds are characterized by reversible Ru(II)–Ru(III) transitions. Further oxidation to Ru(IV) is irreversible. An increasing number of methylene groups in diphosphine ligand or exchange of chlorine by bromine results in the increase of $E_{1/2}$ value similarly as observed for **2**.

CVA curves recorded for complex **3b** at different scan rates, provided in Figure 3, show that no reduction signal is observes after oxidation at 0.8 V versus $Fc|Fc^+$ even with higher scan rates. The dependences of anodic and cathodic currents on a square root scan rate are linear (see Figure 3b) confirming the reversibility of a Ru(II)–Ru(III) transition.

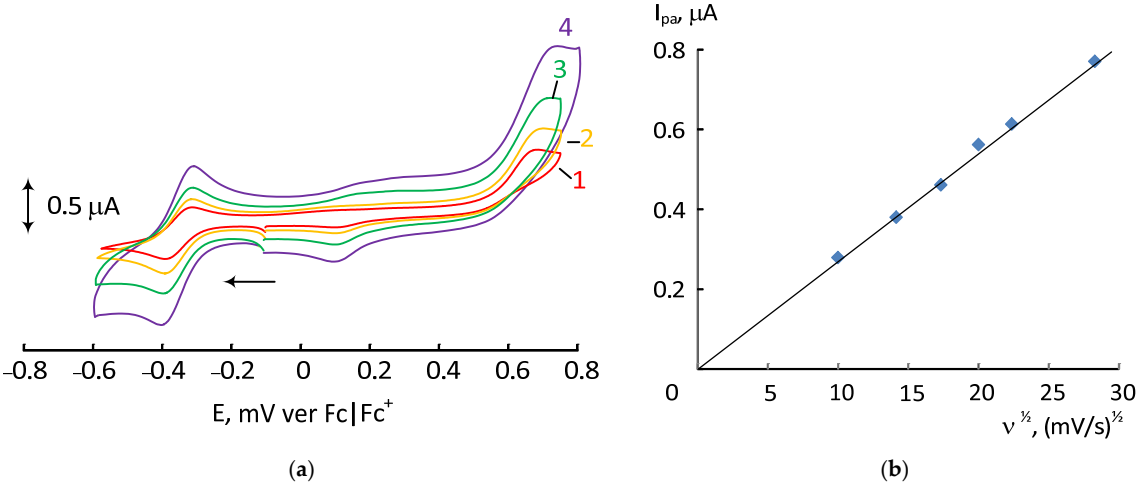

(**a**) (**b**)

Figure 3. (**a**): CVA curves recorded for complex **3b** in 1,2-dichloroethane with 0.2 M n-Bu_4NPF_6 as the supporting electrolyte at 25 °C and different scan rates. [Ru] = 0.003 M. Scan rate: 1—0.1 V/s, 2—0.2 V/s, 3—0.4 V/s, 4—0.8 V/s; (**b**)—the dependence of anodic current on the square root of scan rate (ν) for complex **3b** in the same conditions.

Note, a weak reverse peak of reduction after irreversible oxidation to Ru(IV) state has appeared at 0.1 V. The detailed investigation of the complexes **3a**–**3h** has shown that this peak probably corresponds to the formation of novel complexes capable of reversible transition. According to the CVA curve depicted in Figure 4, irreversible oxidation of **3c** results in the appearance of a reduction peak at 0.13 V. The subsequent oxidation results

in the appearance of a new oxidation peak at 0.18 V, which has not been observed on the oxidation wave in the first cycle. When the potential of the working electrode was kept at 0.8 V for 30 s, the current of the redox wave at 0.18 V has become larger confirming this proposition. Thus, we may conclude that the presence of covalent linkage prevents full decomposition of complexes **3** and **4** after deep oxidation.

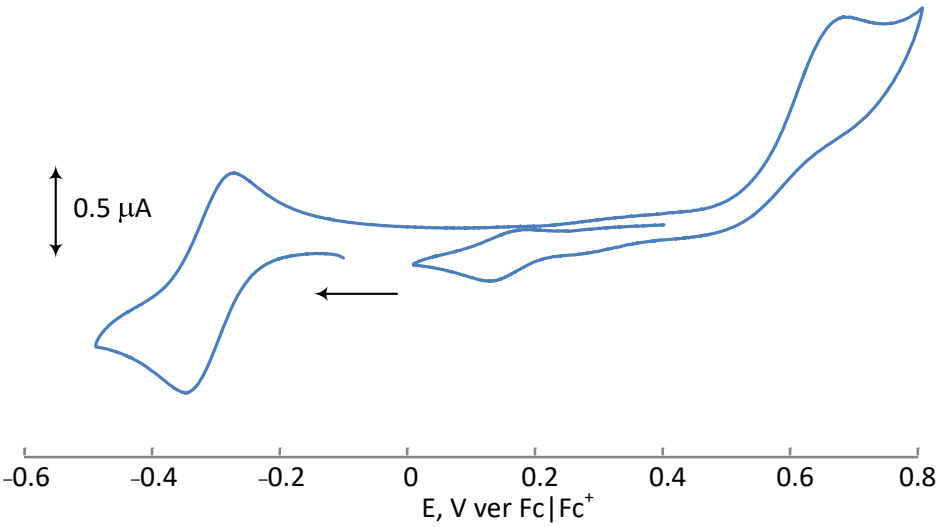

Figure 4. A CVA curve recorded for complex **3c** in 1,2-dichloroethane with 0.2 M n-Bu_4NPF_6 as the supporting electrolyte at 25 °C. [Ru] = 0.003 M. Scan rate: 0.1 V/s.

The oxidation of 18-e complexes of Ru(II) **3i**–**3n** to Ru(III) is also reversible but the potentials of Ru(II)–Ru(III) transition are higher in comparison with 17-e species. Its further oxidation to Ru(IV) is irreversible, while a small reverse peak is observed at 0.6 V (see curve **3i** in Figure 5). Note that triphenylphosphine derivatives of Ru(II) have higher values of redox potentials in comparison with nitrile-based complexes (see curves **3i** and **3m** of Figure 5). Complex **3n** is characterized by a surprisingly low value measured for Ru(II)-Ru(III) transition. It is probably caused by its decomposition with the formation of a dioxygen-containing derivative upon dissolution [28].

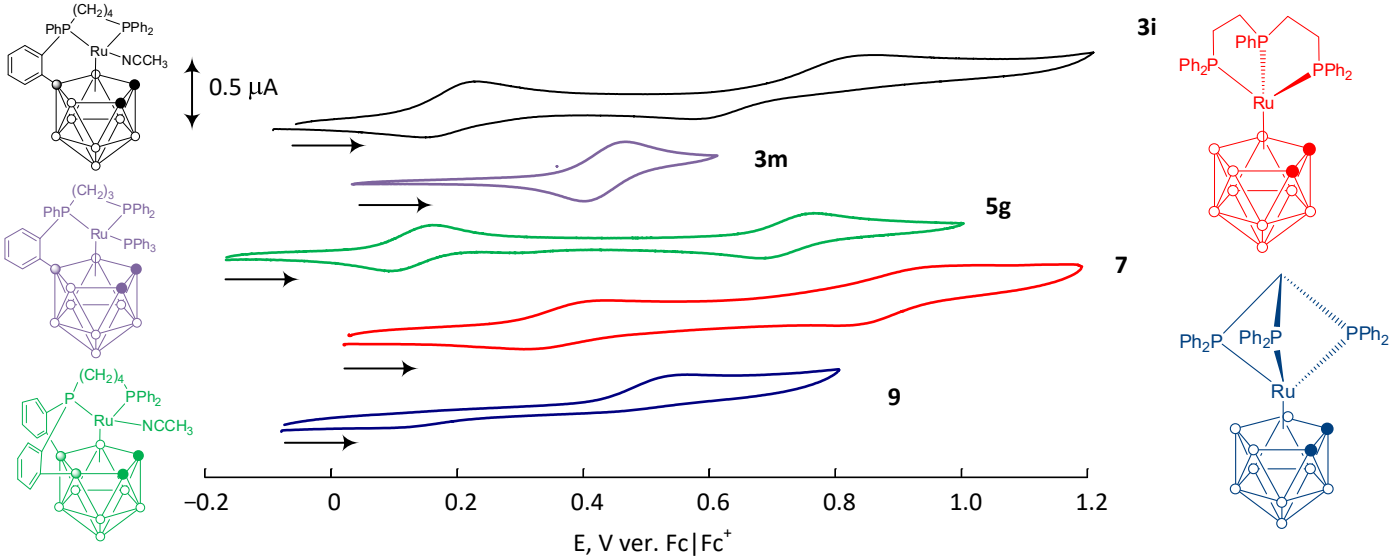

Figure 5. Typical CVA curves were recorded for 18-e complexes of Ru(II) in 1,2-dichloroethane with 0.2 M n-Bu_4NPF_6 as the supporting electrolyte at 25 °C. [Ru] = 0.003 M. Scan rate: 0.1 V/s.

Complexes **3g**, **3h**, **4a** and **4b** contain methyl substituents in the carborane cage. A comparison of the data obtained for these compounds and their unsubstituted analogs

shows that the presence of methyl groups in the structure of carborane ligand results in a decrease of $E_{1/2}$ value. The introduction of the first group results in the decrease of potential by 0.068 V (**3b** and **3g**) while the introduction of the second one decreases the potential only by 0.029 V (**3g** and **3h**). It should be noted that the position of the methyl group in the cage has no significant influence on the electrochemical parameters. The introduction of two methyl groups to carbon atoms in the upper belt of the cage results in a similar decrease of the potential approximately by 0.1 V (**4a**–**4b** and **3a**–**3b**).

Compounds **5a**–**5g** are characterized by two covalent bonds between carborane and diphosphine ligands which significantly increase its stability. The presence of the second *ortho*-cycloboronated fragment surprisingly leads to the reversibility of Ru(III)-Ru(IV) transition. This reversibility is observed for 17-e species **5a**–**5f** (see curve **5b** in Figure 2) and for 18-e complex **5g** (Figure 5). Other dependencies between the complex structure and redox potential values are the same as discussed in the cases of compounds **2**–**4**. The increase of the length of the methylene chain expectedly leads to the increase of $E_{1/2}$ for Ru(II)–Ru(III) transition and also increases $E_{1/2}$ of reversible oxidation to Ru(IV). Methyl substituents in the carborane cage decrease values of $E_{1/2}$ for both transitions.

Comparison of $E_{1/2}$ values measured for complexes **2c**, **3a**, and **5a** shows that the appearance of the first and the second *ortho*-cycloboronated fragments in ruthenacarborane complex decreases its redox potential. A similar tendency is observed for other rows of relative compounds (see Figure 2). Formation of this fragment may be considered as intramolecular introduction of *ortho*-phenylene substituent in the carborane cage. Thus, it correlates with the discussed ability of alkyl substituents to decrease the oxidation potential of ruthenacarboranes.

Compounds **6a**–**6f** have similar structures to the earlier discussed **2a**–**2r** but contain chelate P-O-P ligands which coordinate to ruthenium by two phosphorus atoms. Compounds **6a**–**6c** are 17-e Ru(III) species that undergo reversible reduction to Ru(II) at potential values close to the same of the corresponding bis(diphenylphosphino)alkane derivatives **2b** and **2c**. Its CVA curves are similar to the same of **2d**. Its oxidation to Ru(IV) proceeds irreversible and the Ep_a values significantly depend on the nature of the ligand. The Ni-Xantphos-based complex **6b** has the lowest oxidative stability, while the XantPhos based **6c** is the most stable. Among the 18-e derivatives of Ru(II) **6d**–**6f** only two compounds are capable of reversible oxidation. Its $E_{1/2}$ is typical for complexes with nitrile ligands. Oxidation of **6e** to Ru(III) is fully irreversible due to the low oxidative stability of the Ni-Xantphos ligand.

Ruthenacarboranes **7–9** are 18-e complexes of Ru(II) with triphosphine ligands. Despite the similarity of their structures, they are characterized by different electrochemical behavior. Complex **7** is characterized by two reversible transitions, while the oxidation of **8** and **9** is irreversible (Figure 5). It should be noted that Ep_a values for complex **7** are close to the values observed in the discussed tris-phosphine derivatives **3l**, **3m**, and **2q** (see curves **3m** and **7** in Figure 5).

Compound **10** is a product of interaction **9** with carbon tetrachloride [34]. It is a 17-e complex of trivalent ruthenium. It can also be considered as a derivative of **2a**, where one hydrogen atom is substituted by the PPh_2 group. Its electrochemical properties are similar to the same of **2a**. It also undergoes reversible reduction to Ru(II) and irreversible oxidation to Ru(IV) but at lower potential values than **2a**. The lower $E_{1/2}$ values correlate with donating ability of $-PPh_2$ substituent in the alkyl fragment.

Ruthenacarboranes **11a**–**11e** exhibit 18-e species and contain tridentate nitrogen-based ligands in their structure. Another peculiarity of the mentioned compounds is a so-called *pseudocloso* conformation of carborane ligand with enlarged C-C distance exceeding the sum of covalent radii [35]. These compounds are capable of reversible reduction at potentials close to $E_{1/2}$ of the $Fc|Fc^+$ couple. It should be noted that the introduction of an alkyl substituent to the nitrogen atom results in a change in the value of redox potential. Still, no direct correlation between the nature of the substituent and $E_{1/2}$ value can be observed.

4. Discussion

The analysis of the obtained results allowed us to clearly recognize some patterns and dependences of electrochemical parameters of ruthenacarboranes on their structures which are in good agreement with the earlier mentioned ones.

Most of the studied compounds **2**–**11** undergo reversible Ru(II)-Ru(III) transition while the reversibility of the oxidation to the formal Ru(IV) state depends on the complex structure. The measured potentials of transitions lie in the area typical for Ru(II) | Ru(III) transition [39–42]. At the same time, a comparison of $E_{1/2}$ value for complex **2a** (−0.332 V) with its counterparts containing cyclopentadienyl-anion (Cp, $E_{1/2}$ = −0.015 V) or pentamethylcyclopentadienyl (Cp*, $E_{1/2}$ = −0.190 V) [41] allows us to conclude that dicarbollide ligand is more donating than the mentioned carbocyclic ligands. This ability of parent $[C_2B_9H_{11}]^{2-}$ anion is in good agreement with the observed for its substituted analogs [42] and may be used for the creation of catalysts for processes based on reversible oxidation.

It should be noted that the introduction of alkyl substituents in the carborane cage results in the decrease of $E_{1/2}$ value indicating the donating ability of the substituent. This trend is in good agreement with the observed behavior of sandwich pyrrolyl/dicarbollide cobalt complexes [43] or ruthenium complexes with charge-compensated carborane ligands [42]. The mentioned tendency correlates with the observed dependence of E_{pa} values of ruthenium complexes with substituted η^6-arene on the number of methyl groups [44].

The formation of *ortho*-phenylenecycloboronated fragments in complexes **3**–**5** leads to the decrease of $E_{1/2}$ for Ru(II)-Ru(III) transition. It may be considered as intramolecular substitution in carborane ligand and thus correlates with the previously discussed influence of alkyl substituents. Moreover, the formation of the second *ortho*-cycloboronated link results in the reversibility of the second wave corresponding to the Ru(III)-Ru(IV) transition. Such an effect is similar to the observed reversible oxidation of Ru(η^6-C_6Me_6)-based complexes contrary to the irreversible process for the similar Ru(η^6-C_6H_6) one and may be caused by the decrease of electrode adsorption [44].

Basing on the results of the experiments we may conclude that the increase in the number of methylene units in the alkylidene fragment of the diphosphine ligand results in the increase of the $E_{1/2}$ value for Ru(II)–Ru(III) transition. A similar trend was observed for palladium diphosphine complexes [45] and is probably explained by structural distortions and stabilizing the LUMO in the case of compounds with large bite angles.

According to the provided data, the potential of Ru(II)–Ru(III) transition of the studied ruthenacarboranes **2** varies from −0.439 to +0.389 V versus ferrocene depending on the nature of auxiliary ligands. The comparison of $E_{1/2}$ for the relative Ru(III) complexes with different halogen atoms shows that chlorine-based complex usually displays a lower redox potential than similar complexes with bromine atoms. It should be noted that analogous observation was done for copper complexes with nitrogen-based ligands [46]. Complexes of Ru(II) with nitrile ligands have higher $E_{1/2}$ values in comparison with halogen-based complexes of Ru(II) similar to Cp-based complexes [41]. Ruthenacarboranes containing triphenylphosphine are characterized by the highest oxidation potentials.

Compounds **11a**–**f** with tridentate ligands are classified as *pseudocloso*-ruthenacarboranes. Its reversible Ru(II)-Ru(III) transition have potential close to the corresponding of Ru(CH_3CN)(2,2′-bipyridine)$C_2B_9H_{11}$ (ca 0.05 V ver. Fc | Fc^+, [47], taking into account E(Fc | Fc^+) = 0.10 V versus Ag | $AgNO_3$ [48]).

5. Conclusions

We may conclude that *closo*-ruthenacarboranes, despite similar structures, are very diverse from the point of view of their electrochemical properties. Diamagnetic complexes of Ru(IV) undergo irreversible oxidation. 17-e complexes of Ru(III) undergo reversible reduction to Ru(II) species. Oxidation of 18-e complexes of Ru(II) to Ru(III) species also reverses. The further oxidation of the formed cations towards formal Ru(IV) may be reversible or not depending on the complex structure.

The provided results of electrochemical studies of ruthenacarboranes indicate that Ru(II)-Ru(III) transition is reversible for the major part of the complexes, while the value of potential varies in a wide range depending on the nature of auxiliary phosphine ligand and substituents in the carborane cage. Considering that dicarbollide ligand is more donating than carbocyclic ligands *closo*-ruthenacarboranes seem suitable for application as catalysts for ATRP and other redox processes. Among the studied complexes the compounds of types **3**–**5** with covalently bounded carborane and diphosphine moieties are the most stable and preferable for catalytic applications.

Despite the value of the potential of reversible Ru(II)–Ru(III) transition of ruthenacarboranes may vary in a wide range from −0.501 to 0.389, the found correlations allow proposing the ways of further expanding this range by modification of carborane cage or changing the auxiliary ligand. Moreover, the data provided in Table 2 and the found regularities may be successfully used for tuning other classes of ruthenium complexes for their practical applications.

Author Contributions: Conceptualization, electrochemical study, manuscript writing, supervision, funding acquisition, I.D.G.; synthesis and formal analysis, A.A.K. and A.M.Z. All authors have read and agreed to the published version of the manuscript.

Funding: The work was supported by the Grant of President of Russian Federation (proj. No. MD-1474.2022.1.3).

Data Availability Statement: The data that support the findings of this study are available on request from the corresponding author via e-mail.

Conflicts of Interest: The authors declare no conflict of interest.

References

1. Grimes, R.N. Carboranes in catalysis. In *Carboranes*, 3rd ed.; Academic Press: Cambridge, MA, USA, 2016; pp. 929–944. [CrossRef]
2. Chan, A.P.Y.; Parkinson, J.A.; Rosair, G.M.; Welch, A.J. Bis(phosphine)hydridorhodacarborane derivatives of 1,1′-bis(*ortho*-carborane) and their catalysis of alkene isomerization and the hydrosilylation of acetophenone. *Inorg. Chem.* **2020**, *59*, 2011–2023. [CrossRef]
3. Vinogradov, M.M.; Loginov, D.A. Rhoda- and iridacarborane halide complexes: Synthesis, structure and application in homogeneous catalysis. *J. Organomet. Chem.* **2020**, *910*, 121135. [CrossRef]
4. Zhu, Y.; Hosmane, N.S. Carborane-based catalysts for polymerization of olefins. In *Handbook of Boron Science with Applications in Organometallics, Catalysis, Materials and Medicine. Vol. 2. Boron in Catalysis*; Hosmane, N.S., Eagling, R., Eds.; World Scientific Publishing Europe Ltd.: Singapore, 2018; pp. 117–134. [CrossRef]
5. Stogniy, M.Y.; Erokhina, S.A.; Suponitsky, K.Y.; Markov, V.Y.; Sivaev, I.B. Synthesis and crystal structures of nickel(II) and palladium(II) complexes with o-carboranyl amidine ligands. *Dalton Trans.* **2021**, *50*, 4967–4975. [CrossRef]
6. Teixeira, R.G.; Marques, F.; Robalo, M.P.; Fontrodona, X.; Garcia, M.H.; Crich, G.S.; Vinas, C.; Valente, A. Ruthenium carboranyl complexes with 2,2′-bipyridine derivatives for potential bimodal therapy application. *RSC Adv.* **2020**, *10*, 16266–16276. [CrossRef]
7. Richel, A.; Demonceau, A.; Noels, A.F. Electrochemistry as a correlation tool with the catalytic activities in [$RuCl_2$(p-cymene)(PAr_3)]-catalysed Kharasch additions. *Tetrahedron Lett.* **2006**, *47*, 2077–2081. [CrossRef]
8. Tang, W.; Kwak, Y.; Braunecker, W.; Tsarevsky, N.V.; Coote, M.L.; Matyjaszewski, K. Understanding atom transfer radical polymerization: Effect of ligand and initiator structures on the equilibrium constants. *J. Am. Chem. Soc.* **2008**, *130*, 10702–10713. [CrossRef]
9. Chatterjee, D.; Oszajca, M.; Katafias, A.; van Eldik, R. Electrochemistry of Ru(edta) complexes relevant to small molecule transformations: Catalytic implications and challenges. *Coord. Chem. Rev.* **2021**, *436*, 213773. [CrossRef]
10. Patil-Deshmukh, A.B.; Mohite, S.S.; Chavan, S.S. Ru(II)-polypyridine complexes with alkynyl Schiff base ligand: Influence of π-conjugation, donor/acceptor substituents, and counter anions on electrochemical, luminescence, and catalytic properties. *J. Coord. Chem.* **2020**, *73*, 1028–1044. [CrossRef]
11. Reisner, E.; Arion, V.B.; Guedes da Silva, M.F.C.; Lichtenecker, R.; Eichinger, A.; Keppler, B.K.; Kukushkin, V.Y.; Pombeiro, A.J.L. Tuning of redox potentials for the design of ruthenium anticancer drugs—An electrochemical study of [*trans*-$RuCl_4$L(DMSO)]- and [*trans*-$RuCl_4L_2$]- complexes, where L = imidazole, 1,2,4-triazole, indazole. *Inorg. Chem.* **2004**, *43*, 7083–7093. [CrossRef]
12. Bomben, P.G.; Robson, K.C.D.; Sedach, P.A.; Berlinguette, C.P. On the viability of cyclometalated Ru(II) complexes for light-harvesting applications. *Inorg. Chem.* **2009**, *48*, 9631–9643. [CrossRef]
13. Shahroosvand, H.; Rezaei, S.; Mohajerani, E.; Mahmoudi, M.; Kamyabia, M.A.; Nasiria, S. Key role of ancillary ligands in imparting blue shift in electroluminescence wavelength in ruthenium polypyridyl light-emitting diodes. *New J. Chem.* **2014**, *38*, 5312–5323. [CrossRef]
14. Geiger, W.E. One-electron electrochemistry of parent piano-stool complexes. *Coord. Chem. Rev.* **2013**, *257*, 1459–1471. [CrossRef]
15. von Eschwege, K.G.; Conradie, J. Review of DFT-simulated and experimental electrochemistry properties of the polypyridyl Row-1 Mn, Fe & Co, and Group-8 Fe, Ru and Os MLCT complexes. *Electrochem. Commun.* **2022**, *136*, 107225. [CrossRef]

16. Alexiou, C.; Lever, A.B.P. Tuning metalloporphyrin and metallophthalocyanine redox potentials using ligand electrochemical (E_L) and Hammett (p) parametrization. *Coord. Chem. Rev.* **2001**, *216–217*, 45–54. [CrossRef]
17. Van Caemelbecke, E.; Phan, T.; Osterloh, W.R.; Kadish, K.M. Electrochemistry of metal-metal bonded diruthenium complexes. *Coord. Chem. Rev.* **2021**, *434*, 213706. [CrossRef]
18. Ramesh, G.; Kumar, P.R.; Pillegowda, M.; Periyasamy, G.; Suchetan, P.A.; Butcher, R.J.; Forod, S.; Nagaraju, G. Synthesis, crystal structures, photophysical, electrochemical studies, DFT and TD-DFT calculations and Hirshfeld analysis of new 2,2′:6′,2″-terpyridine ligands with pendant 4′-(trimethoxyphenyl) groups and their homoleptic ruthenium complexes. *New J. Chem.* **2020**, *44*, 11471–11489. [CrossRef]
19. Grishin, I.D.; D'yachihin, D.I.; Piskunov, A.V.; Dolgushin, F.M.; Smolyakov, A.F.; Il'in, M.M.; Davankov, V.A.; Chizhevsky, I.T.; Grishin, D.F. Carborane complexes of ruthenium(III): Studies on thermal reaction chemistry and the catalyst design for atom transfer radical polymerization of methyl methacrylate. *Inorg. Chem.* **2011**, *50*, 7574–7585. [CrossRef]
20. Grishin, I.D.; Zimina, A.M.; Anufriev, S.A.; Knyazeva, N.A.; Piskunov, A.V.; Dolgushin, F.M.; Sivaev, I.B. Synthesis and Catalytic Properties of Novel Ruthenacarboranes Based on nido-[5-Me-7,8-$C_2B_9H_{10}]^{2-}$ and nido-[5,6-Me_2-7,8-$C_2B_9H_9]^{2-}$ Dicarbollide Ligands. *Catalysts* **2021**, *11*, 1409. [CrossRef]
21. Corrigan, N.; Jung, K.; Moad, G.; Hawker, C.J.; Matyjaszewski, K.; Boyer, C. Reversible-deactivation radical polymerization (Controlled/living radical polymerization): From discovery to materials design and applications. *Prog. Polym. Sci.* **2020**, *111*, 101311. [CrossRef]
22. Zhou, Y.N.; Li, J.J.; Wang, T.T.; Wu, Y.Y.; Luo, Z.H. Precision polymer synthesis by controlled radical polymerization: Fusing the progress from polymer chemistry and reaction engineering. *Prog. Polym. Sci.* **2022**, *130*, 101555. [CrossRef]
23. Gagne, R.R.; Koval, C.A.; Lisensky, G.C. Ferrocene as an internal standard for electrochemical measurements. *Inorg. Chem.* **1980**, *19*, 2854–2855. [CrossRef]
24. Kaltenberg, A.A.; Zimina, A.M.; Bashilova, A.D.; Malysheva, Y.B.; Vorozhtsov, D.L.; Piskunov, A.V.; Somov, N.V.; Grishin, I.D. The peculiarities of interaction of 5,6,10-{$Cl(Ph_3P)_2Ru$}-[5,6,10-(μ-H)$_3$-10-H-exo-nido-7,8-$C_2B_9H_8$ with bis(diphenylphosphino)methane and 1,2-bis(diphenylphosphino)benzene. *Russ. Chem. Bull. Int. Ed.* **2014**, *72*, 912–924. [CrossRef]
25. Cheredilin, D.N.; Dolgushin, F.M.; Grishin, I.D.; Kolyakina, E.V.; Nikiforov, A.S.; Solodovnikov, S.P.; Il'in, M.M.; Davankov, V.A.; Chizhevsky, I.T.; Grishin, D.F. Facile method for the synthesis of ruthenacarboranes, diamagnetic 3,3-[$Ph_2P(CH_2)_nPPh_2$]-3-H-3-Cl-closo-3,1,2-$RuC_2B_9H_{11}$ (n = 3 or 4) and paramagnetic 3,3-[$Ph_2P(CH_2)_nPPh_2$]-3-Cl-closo-3,1,2-$RuC_2B_9H_{11}$ (n = 2 or 3), as efficient initiators of controlled radical polymerization of vinyl monomers. *Russ. Chem. Bull. Int. Ed.* **2006**, *55*, 1163–1170. [CrossRef]
26. Grishin, I.D.; D'yachihin, D.I.; Turmina, E.S.; Dolgushin, F.M.; Smol'yakov, A.F.; Piskunov, A.V.; Chizhevsky, I.T.; Grishin, D.F. Mononuclear *closo*-ruthenacarborane complexes containing a rare eight-membered metal-diphosphine ring. *J. Organomet. Chem.* **2012**, *721–722*, 113–118. [CrossRef]
27. D'yachihin, D.I.; Grishin, I.D.; Piskunov, A.V.; Godovikov, I.A.; Kostukovich, A.Y.; Smol'yakov, A.F.; Dolgushin, F.M.; Chizhevsky, I.T.; Grishin, D.F. Efficient methods for the preparation of bromine-containing *exo-nido*- and *closo*-ruthenacarborane clusters. *Russ. Chem. Bull. Int. Ed.* **2014**, *63*, 2325–2333. [CrossRef]
28. Zimina, A.M.; Knyazeva, N.A.; Balagurova, E.V.; Dolgushin, F.M.; Somov, N.V.; Vorozhtsov, D.L.; Malysheva, Y.B.; Grishin, I.D. Revising the chemistry of κ^2-dppe-*closo*-$RuC_2B_9H_{11}$ fragment: Synthesis of novel diamagnetic complexes and its transformations. *J. Organomet. Chem.* **2021**, *946–947*, 121908. [CrossRef]
29. Penkal, A.M.; D'yachihin, D.I.; Somov, N.V.; Shchegravina, E.S.; Grishin, I.D. Synthesis of novel *closo*-carborane complexes of ruthenium (II) with triphenylphosphine or acetonitrile ligands via reduction of paramagnetic Ru(III) derivatives. *J. Organomet. Chem.* **2018**, *872*, 63–72. [CrossRef]
30. Penkal, A.M.; Somov, N.V.; Shchegravina, E.S.; Grishin, I.D. Ruthenium Diphosphine Closo-C_2B_9-Carborane Clusters with Nitrile Ligands: Synthesis and Structure Determination. *J. Clust. Sci.* **2019**, *30*, 1317–1325. [CrossRef]
31. Grishin, I.D.; Agafonova, K.S.; Kostyukovich, A.Y.; D'yachihin, D.I.; Godovikov, I.A.; Dolgushin, F.M.; Grishin, D.F.; Chizhevsky, I.T. Synthesis of metallacarborane ruthenium(II) and ruthenium(III) complexes with chelate 1,3-bis(diphenylphosphino)propane ligand and their mutual transformation in one-electron redox reactions. *Russ. Chem. Bull. Int. Ed.* **2016**, *65*, 1574–1579. [CrossRef]
32. Gritzner, G.; Kůta, J. Recommendations on reporting electrode potentials in nonaqueous solvents: IUPC commission on electrochemistry. *Pure Appl. Chem.* **1984**, *56*, 461–466. [CrossRef]
33. Zimina, A.M.; Somov, N.V.; Malysheva, Y.B.; Knyazeva, N.A.; Piskunov, A.V.; Grishin, I.D. 12-Vertex *closo*-3,1,2-ruthenadicarbadodecaboranes with chelate POP-ligands: Synthesis, X-ray study and electrochemical properties. *Inorganics* **2022**, *10*, 206. [CrossRef]
34. Kaltenberg, A.A.; Somov, N.V.; Malysheva, Y.B.; Knyazeva, N.A.; Piskunov, A.V.; Grishin, I.D. Novel carborane complexes of ruthenium with tridentate phosphine ligands: Synthesis and application in Atom Transfer Radical Polymerization. *J. Organomet. Chem.* **2020**, *917*, 121291. [CrossRef]
35. Kaltenberg, A.A.; Somov, N.V.; Malysheva, Y.B.; Vorozhtsov, D.L.; Grishin, I.D. Synthesis of novel *pseudocloso* ruthenacarboranes based on an unsubstituted *nido*-$C_2B_9H_{11}{}^{2-}$ ligand. *Eur. J. Inorg. Chem.* **2021**, *2021*, 4868–4874. [CrossRef]
36. Núñez, R.; Tarrés, M.; Ferrer-Ugalde, A.; Fabrizi de Biani, F.; Teixidor, F. Electrochemistry and photoluminescence of icosahedral carboranes, boranes, metallacarboranes, and their derivatives. *Chem. Rev.* **2016**, *116*, 14307–14378. [CrossRef]

37. Chizhevsky, I.T.; Lobanova, I.A.; Petrovskii, P.V.; Bregadze, V.I.; Dolgushin, F.M.; Yanovsky, A.I.; Struchkov, Y.T.; Chistyakov, A.L.; Stankevich, I.V.; Knobler, C.B.; et al. Synthesis of mixed-metal (Ru−Rh) bimetallacarboranes via *exo-nido*- and *closo*-ruthenacarboranes. Molecular structures of (η^4-C_8H_{12})Rh(μ-H)Ru(PPh_3)$_2$(η^5-$C_2B_9H_{11}$) and (CO)(PPh_3)Rh(μ-H)Ru(PPh_3)$_2$(η^5-$C_2B_9H_{11}$) and their anionic *closo*-ruthenacarborane precursors. *Organometallics* **1999**, *18*, 726–735. [CrossRef]
38. Dierkes, P.; van Leeuwen, P.W.N.M. The bite angle makes the difference: A practical ligand parameter for diphosphine ligands. *J. Chem. Soc. Dalton Trans.* **1999**, *10*, 1519–1530. [CrossRef]
39. Kovalski, E.; Korb, M.; Hildebrandt, A. Synthesis, electrochemistry, and optical properties of half-sandwich ruthenium complexes bearing triarylamine-anthracenes. *Eur. J. Inorg. Chem.* **2018**, *2018*, 671–675. [CrossRef]
40. Fox, M.A.; Roberts, R.L.; Khairul, W.M.; Hartl, F.; Low, P.J. Spectroscopic properties and electronic structures of 17-electron half-sandwich ruthenium acetylide complexes, [Ru(C≡CAr)(L_2)Cp′]$^+$ (Ar = phenyl, p-tolyl, 1-naphthyl, 9-anthryl; L_2 = (PPh_3)$_2$, Cp′ = Cp; L_2 = dppe; Cp′ = Cp*). *J. Organomet. Chem.* **2007**, *692*, 3277–3290. [CrossRef]
41. Morandini, F.; Dondana, A.; Munari, I.; Pilloni, G.; Consiglio, G.; Sironi, A.; Moret, M. Pentamethylcyclopentadienyl ruthenium(II) complexes containing chiral diphospines: Synthesis, characterisation and electrochemical behaviour. X-ray structure of (η^5-C_5Me_5)Ru{(S,S)-$Ph_2PCH(CH_3)CH(CH_3)PPh_2$}Cl. *Inorg. Chim. Acta* **1998**, *282*, 163–172. [CrossRef]
42. Tutusaus, O.; Vinas, C.; Nunez, R.; Teixidor, F.; Demonceau, A.; Delfosse, S.; Noels, A.F.; Mata, I.; Molins, E. The modulating possibilities of dicarbollide clusters: optimizing the Kharasch catalysts. *J. Am. Chem. Soc.* **2003**, *125*, 11830–11831. [CrossRef]
43. Llop, J.; Viñas, C.; Teixidor, F.; Victori, L.; Kivekäs, R.; Sillanpää, R. Redox potential modulation in mixed sandwich pyrrolyl/dicarbollide complexes. *Inorg. Chem.* **2002**, *41*, 3347–3352. [CrossRef]
44. Auzias, M.; Therrien, B.; Süss-Fink, G.; Štěpnička, P.; Han, P.; Ang, W.H.; Dyson, P.K. Ferrocenoyl pyridine arene ruthenium complexes with anticancer properties: synthesis, structure, electrochemistry, and cytotoxicity. *Inorg. Chem.* **2008**, *47*, 578–583. [CrossRef]
45. Raebiger, J.W.; Miedaner, A.; Curtis, C.J.; Miller, S.M.; Anderson, O.P.; DuBois, D.L. Using ligand bite angles to control the hydricity of palladium diphosphine complexes. *J. Am. Chem. Soc.* **2004**, *126*, 5502–5514. [CrossRef]
46. Qiu, J.; Matyjaszewski, K.; Thouin, L.; Amatore, C. Cyclic voltammetric studies of copper complexes catalyzing atom transfer radical polymerization. *Macromol. Chem. Phys.* **2000**, *201*, 1625–1631. [CrossRef]
47. Jelliss, P.A.; Mason, J.; Nazzoli, J.M.; Orlando, J.H.; Vinson, A. Synthesis and characterization of ruthenacarborane complexes incorporating chelating n-donor ligands: Unexpected luminescence from the complex [3-CO-3,3-{k^2-$Me_2N(CH_2)_2NMe_2$}-*closo*-3,1,2-$RuC_2B_9H_{11}$]. *Inorg. Chem.* **2006**, *45*, 370–385. [CrossRef]
48. Vorotyntsev, M.A.; Casalta, M.; Pousson, E.; Roullier, L.; Boni, G.; Moise, C. Redox properties of titanocene-pyrrole derivative and its electropolymerization. *Electrochim. Acta* **2001**, *46*, 4017–4033. [CrossRef]